Ordered growth of Ge island clusters on strain-engineered Si surfaces

M. De Seta,[1] G. Capellini,[1,*] and F. Evangelisti[1,2]
[1]*Dipartimento di Fisica "E. Amaldi", Università degli Studi Roma Tre, via della Vasca Navale 84, I-00146 Roma, Italy*
[2]*Istituto di Fotonica e Nanotecnologie, Consiglio Nazionale delle Ricerche, Via Cineto Romano 42, I-00156 Roma, Italy*
(Received 17 March 2004; revised manuscript received 16 September 2004; published 15 March 2005)

We report on the tailoring of the stress field distribution at the surface in a multilayered Ge/Si system in order to have a spontaneous ordering of the self-assembled islands in multi-island *clusters*. These clusters are ordered along [100]-[010] directions and arranged in a simple planar lattice. We investigate the evolution, from nucleation to ripening, of the Ge islands inside the clusters for two different stress modulations at the surface. The control over the stress at the surface has been obtained by tuning the last Si spacer layer thickness in a stacked-island multilayered structure. An appropriate selection of this spacer layer thickness allowed us to modulate the stress in two different limits of strong and weak island-island vertical interaction. We demonstrate that the stress modulation can be used to influence the island growth dynamics in order to induce an ordered spatial position of islands inside the cluster, to reduce the island size and to narrow the island size distribution.

DOI: 10.1103/PhysRevB.71.115308 PACS number(s): 81.16.Dn, 68.65.Hb, 68.55.Jk

INTRODUCTION

Self-assembled semiconductor quantum dots are interesting candidates for implementing new devices based on the bottom-up approach to nanotechnology. These nanometric particles are obtained through self-organization driven by the strain field resulting from the lattice mismatch present at the interface between epilayer and substrate in semiconductor heteroepitaxy.[1] The Ge/Si islands formed under the Stranski-Krastanov (SK) growth regime are a typical example of such a process and could be of particular interest in Si-compatible micro- and opto-electronics.[2]

As pointed out by Schmidt and coworkers,[3] for real use of the self-assembled islands, four degrees of order have to be controlled: (i) orientation, (ii) shape, (iii) size, and (iv) spatial positioning. The first two levels of order are usually obtained during heteroepitaxial growth, given the anisotropy of the elastic properties and surface energy of the most common semiconductors.[4–6] Controlling size and size homogeneity is a more difficult task even though it can be partially accomplished by acting on the deposition parameters that influence the island growth.[7–10] The poor control over the island spatial position and order is the main obstacle to their use in the fabrication of electronic devices. Indeed, the possibility of positioning a nanoparticle with high accuracy is of paramount importance in the device fabrication process.

It is well known that a high degree of vertical order and island homogeneity is obtained when several island layers separated by a spacer layer are stacked on top of each other. The buried islands induce into the spacer layer a strain energy modulation, which influences the island nucleation process in subsequent layers.[11,12] As a result, the adatom surface diffusivity is such that a higher Ge adatom concentration is present in those regions where the Si lattice is tensile strained and the islands nucleate preferentially in these regions.[11–15] Furthermore, the elastic anisotropy of the Ge/Si systems also leads to a planar ordering of the islands along the in-plane [100]-[010] crystalline directions.[16,17] This order is enhanced by the vertical interaction between islands.[11,12]

We have recently demonstrated[15] that a further level of ordering can be introduced in the island organization by tailoring the strain distribution at the surface and the deposition conditions. Planar lattices of clusters of islands were obtained. The clusters were composed of a few Ge nanosized islands, regularly arranged inside the cluster itself. Thus, a variety of ordered planar configurations can be obtained without the use of lithographic processes.

It is the main purpose of this paper to discuss the Ge island evolution, from nucleation to ripening, in this type of sample. We have compared the evolution of the island clusters as a function of the deposited material for different intensities of the strain at the surface. Such a strain variation was obtained by changing the thickness of the last Si spacer layer in the multilayered structure. An appropriate selection of this thickness allowed us to modulate the stress at the surface in two different limits of strong and weak island-island vertical interactions. We will also show that the stress modulation can be used in order to modify the island growth dynamics with the result of reducing the island size and narrowing the size distribution.

EXPERIMENTAL DETAILS AND RESULTS

The sample growth has been carried out in an ultra-high-vacuum chemical vapor deposition (CVD) reactor whose base pressure was in the low 10^{-10} Torr range. The Si(001) substrates were cleaned in H_2 atmosphere at 1100°C. Prior to sample deposition, a 500 nm thick Si buffer layer was grown from silane at a deposition temperature $T_{dep}=750\,^{\circ}\mathrm{C}$.

The morphological characterization of the samples was performed by means of an ambient Park Scientific Instruments CP atomic force microscope (AFM) operating in contact mode using a silicon tip having a high aspect ratio and a small radius (5 nm). In order to have a good trade-off between lateral resolution and statistical reliability, we have acquired AFM topographies with a lateral step of 1.4 nm. Convolution effects resulting from the finite tip size were corrected.

In order to obtain the ordered distribution of strain that would originate the island clusters, we first obtained an or-

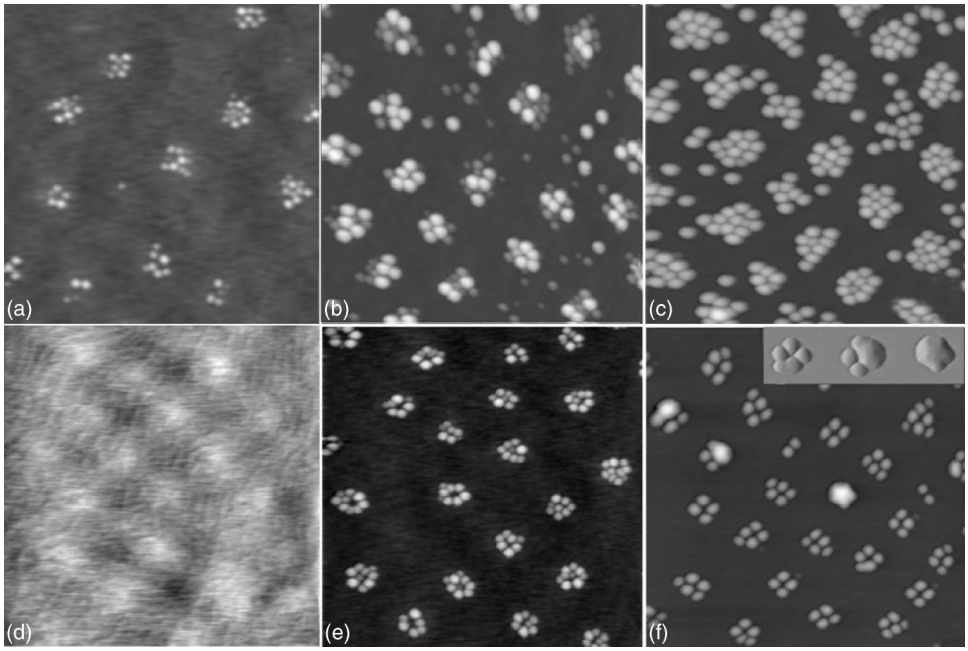

FIG. 1. 2×2 μm^2 AFM images of Ge islands deposited on multilayer templates. Panels (a), (b), and (c) 65 nm thick topmost silicon layer and deposition times of 18, 25, and 50 s, respectively. Panels (d), (e), and (f) 35 nm thick topmost silicon layer and deposition times of 9, 18, and 50 s, respectively. In the (f) panel inset three island clusters, containing relaxed domes at different stages of their evolution are displayed in differential mode. Image sides are oriented along the $\langle 011 \rangle$ directions. Notice that the vertical gray-tone scale has been adjusted differently in each panel in order to better display the characteristic features of the imaged sample.

dered array of Ge islands by exploiting the self-ordering occurring in the growth of island multilayers. To this purpose, a multilayer structure made by repeating ten periods of 7-monolayer-thick (ML) Ge islands deposited on top of a 60 nm thick Si spacer layer has been grown on Si(001) substrate at a temperature of 750°C. For the Ge layer deposition we used germane without a carrier gas at a pressure of 0.4 mTorr. Hereafter, we will refer to such a structure as the *template*.

Before the subsequent Si layer deposition, each Ge-island layer of the template was composed of strained multifaceted islands (domes) having a mean base width $b_m = 190$ nm and height $h_m = 35$ nm. Due to Si-Ge intermixing and strain redistribution, the subsequent Si deposition modifies the dome morphology leading to a flatter mesa-like shape.[18] As determined from transmission electron microscopy (TEM),[15] the mesas have a top facet whose width f is about 45% of the base width b (which is typically 220 nm), a sidewall contact angle $\theta = 10°$, and a height $h = 10$ nm. The analysis of the template structure performed by means of TEM and AFM has shown that the Ge islands form an in-plane ordered square lattice aligned along the [100]-[010] crystallographic directions. The in-plane lattice parameter is $P = 350 \pm 30$ nm, as determined by averaging the two-dimensional Fourier transform of four AFM images, each being 100 μm^2 wide. To this purpose, about 7000 nearest-neighbor island distances were taken into account. Given the island vertical alignment, the template results in a tetragonal superlattice, whose off-plane (001) lattice parameter coincides with the spacer layer thickness (60 nm).

The samples have been completed by depositing Si layers of different thicknesses on the template at a deposition temperature of 750° C. On top of the last Si layer, the desired Ge island layer was eventually grown at a deposition temperature of 600° C. The different spacer layer thicknesses allowed us to change in a controlled manner the strain field profile on the topmost Si surface.[11,12,15] On the other hand, the lower deposition temperature used for the top Ge layer allowed us to obtain Ge islands whose size was appreciably smaller than the Ge islands underneath,[19] i.e., smaller than the typical extension of the stress field at the surface.[12]

In Figs. 1(a)–1(c) we show AFM images of three samples prepared by depositing on the template a 65 nm thick Si spacer layer followed by Ge depositions lasting 18, 25, and 50 s, respectively. This sample set is referred to as series A in the following. In Figs. 1(d)–1(f) we show AFM images of three samples having a 35 nm thick Si spacer layer and Ge deposition times of 9, 18, and 50 s, respectively (series B). It is apparent in Fig. 1 that in both series, the islands are assembled in clusters whose location follows the arrangement of the Ge islands in the template and which exhibit a remarkable long-range order. It is also apparent that the order is appreciably improved in the B series, where a regular arrangement of the islands inside the clusters is clearly visible.

The Ge islands on the surface, being deposited at 600°C and not capped by a silicon layer, suffered less intermixing with respect to those buried into the template. Therefore, their typical size (about 60–80 nm) is smaller than the typical size of the template islands and much smaller than the extension of the stress field at the surface.[12]

As further information, we report in Fig. 2 the average diameter Δ of the clusters and the total material deposited in form of islands as a function of Ge deposition time. We define an island cluster as a topological structure formed by at least two adjacent islands having their nearest-neighbor distance smaller than twice the average base width of the two islands.[15] This means that the clusters are made by islands in nearly mutual contact. The cluster diameter Δ is defined as the diameter of a circle having a surface equivalent to that delimited by the perimeter that includes all the islands of the cluster itself. We see in Fig. 2 that Δ changes appreciably from 170 nm to a saturation value of 260 nm in series A, while it varies only slightly in series B.

In order to describe the cluster ordering more quantitatively, we report in Fig. 3(a) the distribution of the polar

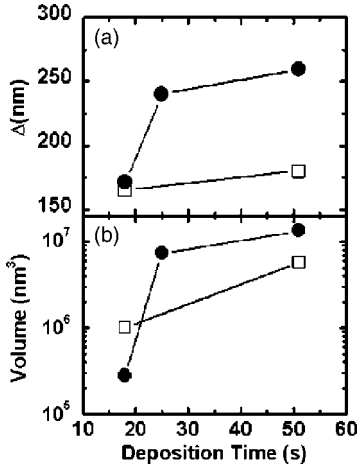

FIG. 2. (a) Mean diameter Δ of the island clusters as a function of Ge deposition time for series A (closed circles) and series B (open squares) samples. (b) Total volume of the Ge islands as a function of deposition time.

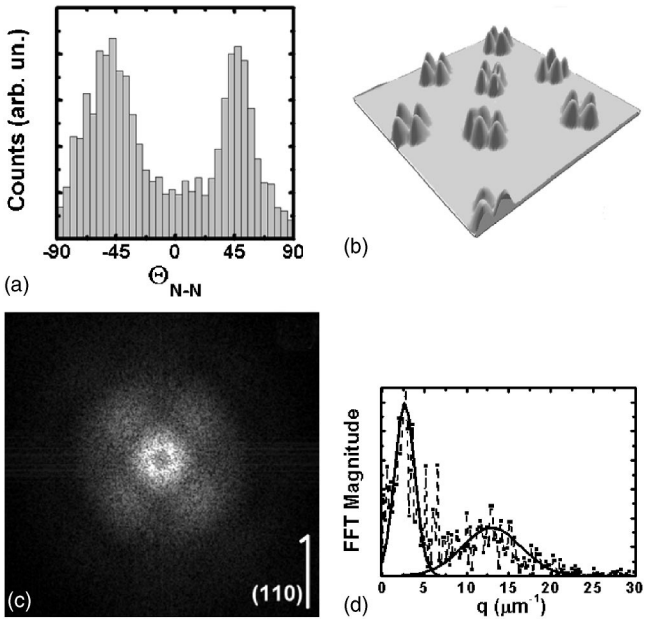

FIG. 3. (a) Measured polar angle defining the angular position of the nearest neighbors of each cluster of the sample shown in Fig. 1(f). The reference direction is the (110) direction. (b) Three-dimensional rendering of an AFM scan of the sample of Fig. 1(f) (scan size 1 μm, scan oriented along the (110) direction). (c) Fast Fourier transform of 100 μm^2 wide AFM scans of the sample of Fig. 1(f). The short-range ordering along the [100]-[010] directions is evidenced by the presence of outer loci in the spectrum. The vertical (intensity) scale of this panel has been optimized in order to evidence the short-range order. (d) Radial intensity profile obtained averaging the Fourier transform amplitude along the [100], [010], [-100], and [0-10] directions.

angle, which defines the angular position of the nearest neighbors of each cluster. The data have been obtained from the analysis of the nearest neighbors of more than 2500 clusters of the sample of Fig. 1(f). The center of mass of the cluster has been taken as the cluster position, and the (110) crystallographic direction has been chosen as reference direction. The long-range ordering of the island clusters along the *soft* [100]-[010] directions is evidenced by the narrow distributions centered at −45° and 45° in Fig. 3(a) and by the presence of four peaks in the two-dimensional Fourier transform of the AFM image presented in Fig. 3(c), located along the ⟨100⟩ equivalent directions at a distance from the origin $q_{long}=2.8\ \mu m^{-1}$ [Fig. 3(d)]. This corresponds to an average distance between the center of mass of neighboring clusters of about 360 nm, very close to the in-plane distance $P=350$ nm existing between adjacent islands in the template. The centers of mass of the clusters are thus arranged in a square lattice identical to those observed in the last layer of the underlying template. The coincidence between the spatial location of the clusters and that of the islands in the template was evidenced by cross-sectional TEM analysis.[15]

We now illustrate the morphology of the islands inside the clusters and their evolution as a function of deposition time. The island characteristics (base width, height, etc.) were determined by means of a quantitative analysis performed on statistically significant sample areas by using the software spip™. About 1000 islands per sample were investigated.

As for the series A, after nucleation on the wetting layer (WL), small pyramids with aspect ratio $\alpha<0.1$ develop in those surface regions where the Si is tensilely deformed [Fig. 1(a)]. The aspect ratio is defined as the ratio between the island height and the island base width b, i.e. the square root of the island base area. The mean value of b has been measured to be 40 nm, while the relative width of its distribution, i.e., the ratio between the standard deviation and the mean value of b, was found to be 0.30. At this early stage, very few islands nucleate and develop outside the *clusters*. To quantify this observation, we report in Fig. 4(a) the growth selectivity S, defined as the ratio between the number of islands inside the clusters and the total number of islands. S is ∼1 at this stage of the growth. Upon increasing the deposited material [Figs. 1(b), 1(c), and 2(a)], the diameter of the clusters, as well as the number of islands forming the clusters, increases. For a deposition time of 25 s, several islands are present on surface regions outside the clusters and the selectivity drops to $S=0.88$. As for their morphology, it is found that the islands exhibit a bimodal distribution of sizes. This bimodal distribution is a signature of the morphological transition from strained pyramids to strained domes.[7]

The fraction of pyramids and domes inside and outside the clusters is reported in Fig. 4 (panels b and c, respectively) as a function of the deposition time. At 25 s deposition time, a similar number of pyramids and domes is present inside the clusters, while 85% of islands outside the clusters are pyramids (Fig. 4).

A further deposition of material (50 s sample) entails a very small increase of the number of islands located outside the clusters. Indeed, the selectivity S is 0.87, negligibly smaller than the 25 s sample value. However, the disappearance of the pyramids and the presence of domes are observed at this deposition time. As can be seen in Fig. 4, a monomodal distribution of domes is present inside and outside the clusters. Domes inside and outside the clusters differ slightly. The mean base size is $b=63$ nm and the aspect ratio is $\alpha=0.18$ for the domes inside the clusters, while $b=81$ nm and $\alpha=0.15$ for domes outside the clusters.

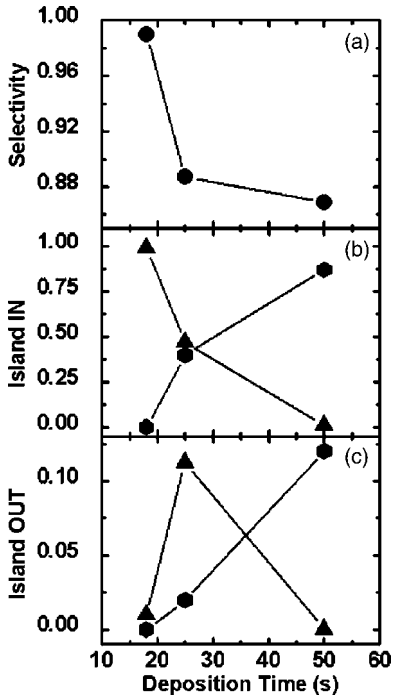

FIG. 4. (a) Growth selectivity, (b) relative abundance of strained Ge pyramids (triangles) and domes (hexagons) inside the clusters, and (c) relative abundance of strained Ge pyramids (triangles) and domes (hexagons), outside the clusters. The above quantities plotted as a function of Ge deposition time pertain to the series A samples.

The different features of the series B, where the Si spacer layer is reduced to 35 nm, highlight the strong effect of reducing the spacer layer thickness. A detailed analysis of the AFM images of this series [Figs. 1(d)–1(f)] show that almost all the islands are located inside the clusters independently of the deposition time; i.e., the selectivity S is greater than 0.98 for all the samples of this series. Furthermore, the diameter of the clusters is smaller than in the series A and varies only slightly with the amount of deposited material (open symbols in Fig. 2).

Figure 1(d) shows that, over a deposition period of 9 s, the Ge WL grows mainly in the surface regions above the template buried islands, as evidenced by the regularly aligned mounds (brighter gray tone). As the deposition proceeds [$t_{dep}=18$ s, Fig 1(e)] the islands develop as square-based pyramids, similarly to series A. The island size distribution in this sample has been measured to be monomodal (pyramids only) with a mean base width $b=45$ nm and mean aspect ratio $\alpha=0.085$. The relative widths of the distributions of the island bases and aspect ratios are 0.19 and 0.15, respectively. We point out that a similar amount of Ge, deposited in the same condition on a bare silicon substrate, results in a multimodal distribution of islands with the coexistence of pyramids and domes.[7]

Upon increasing the deposited material ($t_{dep}=50$ s) the pyramids transform into domes having $b=58$ nm and $\alpha=0.22$. A strong tendency toward an ordered disposition of the islands inside the cluster becomes evident [Fig. 1(f)]. The strained domes are arranged along the [100]-[010] directions with a high degree of order. This ordering is clearly visible in the three-dimensional rendering of an AFM image taken on the same sample and displayed in Fig. 3(b). A quantitative evidence of this short-range (*intracluster*) ordering is given by the presence of outer loci in the spectrum of the two-dimensional Fourier transform of the AFM images [Fig. 3(c)]. These loci, oriented along the ⟨100⟩ equivalent directions, are centered at $q_{short}=13\ \mu m^{-1}$ [Fig. 3(d)]. This value corresponds to a spatial periodicity of about 75 nm, very close to the average base width of the strained domes in the clusters.

Contrary to the A series, plastic relaxation and island coalescence take place inside the clusters before island nucleation occurs outside the clusters. In the inset of Fig. 1(f) we display three clusters at different stages of their relaxation/ripening process. Once one of the strained islands transforms into a relaxed dome, it becomes a preferred site for the adatom attachment and evolves faster than the surrounding islands. The relaxed dome will eventually invade the whole cluster area. We point here out that, even at this late stage of the growth within the cluster regions, no island nucleates in regions outside the clusters.

DISCUSSION

In the Stranski-Krastanov growth on a homogeneous surface, adatom diffusion and the consequent nucleation are random processes. Quite to the contrary, in an island multilayer the adatom dynamics is influenced by the stress field $\sigma(x,y)$ originated by the lattice mismatch existing between the Ge buried islands and the Si surrounding matrix. As a matter of fact, the activation energy for the adatom diffusion depends linearly on the strain energy density. The adatom diffusivity and the chemical potential both depend on the position (x,y), being lower (higher) where the stress energy at the surface is smaller (larger). This sets up an effective adatom concentration gradient that drives biased diffusion toward surface regions located on top of the underlying islands of the template.[13,14] As for the spatial distribution of the strain, it results[11,12,14] that the Si lattice is tensilely strained in a columnar region lying on top of the buried island. Upon increasing the thickness of the Si spacer layer, the width of the tensilely strained region increases, while the intensity of the stress at the surface decreases. Beyond the boundary of the tensile region, a transition zone exists where the Si lattice is compressively strained. Eventually, further away from the buried island, the Si lattice is completely relaxed.

It has been shown that the stress field $\sigma(x,y)$ generated at the surface by buried islands can be approximated by simple analytic models using the linear elasticity theory.[11,16] An analytical expression for the stress profile at the free surface of the capped template is obtained by modeling the array of buried islands as point-like inclusions generating a dipole-like strain field into the Si matrix. However, in order to be in agreement with the actual stress field as calculated by means of large-scale molecular dynamics technique, fitting parameters must be introduced into this analytical solution for a point-like force-dipole.[16] The fitting parameters account for the actual extension and shape of the buried islands.

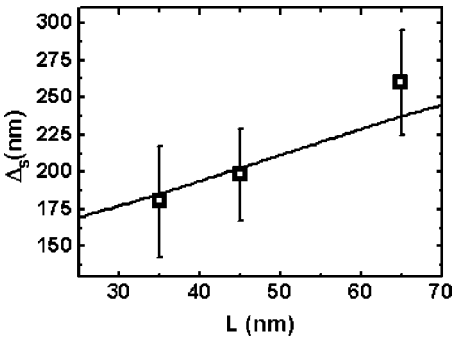

FIG. 5. Measured cluster-width saturation value Δ_S as a function of the Si spacer layer thickness L (open squares) and calculated width of the Si tensile region on the sample surface as a function of L (solid line).

Since our experimental results provide an estimate of the cluster dimensions, which, in turn, is closely related to the extension of the strained regions at the surface, we have a convenient way to derive from the experiment the appropriate parameter for the more suitable analytical model. To this aim, we have fitted the measured cluster-width saturation value Δ_S, as a function of the spacer layer thickness using the analytical expression of the strain field caused by a rectangular buried island, as derived by Liu and coworkers.[12] The saturation value Δ_S has been defined as the cluster diameter at the beginning of the island coalescence inside the cluster. The base width b_{eff} of the rectangular buried island was used as the fitting parameter.

The results are shown in Fig. 5. The best agreement with the experimental values was obtained for $b_{\text{best}}=130$ nm. The obtained value is smaller than the observed (TEM measurements) typical base width of the buried islands (about 220 nm), but is very close to the width of the top facet (about 100 nm) of the island themselves. This fact is not surprising for different reasons.

First of all, the top facet is the part of the island closer to the surface and, as a consequence, its contribution will be the most relevant. Moreover, it is well known that a buried island is richer in Ge close to the top and richer in Si close to the base and that the island is nearly fully lattice matched to Si at the base level and relaxes close to the top.[20–22] As a consequence the "top-central" part of the island is more effectively stressing the surrounding Si matrix than the base boundary does. The "removal" of the contribution of the island bottom corners leads to an "effective" island shape similar to the rectangular one used by Liu *et al.*[12]

We now discuss the island evolution observed in series A. The features of the 18 s sample [Fig. 1(a)] suggest that in a 65 nm thick spacer layer, the stress modulation at the surface is intense enough to determine the nucleation and evolution of small pyramids in the strained regions only. The absence of nucleation outside the cluster regions implies that the mean separation between adjacent strain energy wells is smaller than the Ge adatom mean diffusion length.[23] Furthermore, the islands first nucleate and develop at the center of the stressed region. The diffusivity in the smooth strain energy well is therefore large enough to allow the adatoms to reach the potential well minimum.[24]

As the growth proceeds, the stress field at the surface is affected by the strain contribution of the evolving islands themselves.[8,25] As a result, the new islands nucleate at the cluster boundary. Once the Si tensile regions are filled, the adatoms' strain-driven diffusion is reduced and, in a second stage of the growth, islands nucleate outside the clusters. This two-step scenario accounts for the different dome versus pyramids density ratio observed inside and outside the clusters.

The preferential nucleation of islands inside the clusters results in a high growth rate and a high island density there. By measuring the cluster volume as a function of the deposition time we have evaluated a *local* growth rate of about 70 ML/min and an island density 3.5×10^{10} cm^{-2} inside the cluster regions. It is interesting to note that the mean sizes of the strained domes, equal to 63 nm inside the cluster regions and to 81 nm outside, are comparable with those of domes obtained at high (100 ML/min) and low (4 ML/min) growth rates, respectively, in the deposition on unstrained Si surfaces at similar island densities.[7] This observation confirms a previous finding that the island-island interaction reduces the island size[7] and that, in turn, the island size inside the clusters is tuned by the island-island interaction.

Quite to the contrary to what happen in the series A, we have seen that in the series B the strain modulation at the surface is intense enough that no island nucleation occurs outside the cluster regions and that the islands inside the clusters evolve until plastic relaxation and island coalescence take place still without evidence of nucleation outside the clusters. On the basis of this different capability of gathering the islands in clusters, the strain modulation present on the top surface of a 65 nm and 35 nm thick Si spacer layer can be considered as representative of "weak" and "strong" nucleation regimes, respectively.

A second peculiar feature of the series B samples is that the island clusters have, at their early stage, a corral-like shape [Fig. 1(e)]. This characteristic implies that the island nucleation does not begin at the center of the tensilely strained regions. Furthermore, the cluster width is only slightly dependent on the amount of deposited material, as observed in Fig. 2(a). Within the framework of the biased diffusivity model proposed by Xie *et al.*[14] these findings suggest the presence of a local maximum of the strain energy density in the center of the tensilely strained region. The strain energy minimum would acquire a ring-like shape where the nucleation would take place, leading to the observed cluster shape. Recent first-principles atomistic calculations do indeed show the presence of a local maximum of the strain energy density at the surface, corresponding to the center of a mesa-shaped buried island for thin Si spacer layers ($L\approx30$ nm).[26]

It is worth pointing out, however, that the above characteristics can also be accounted for by the model of kinetically limited "biased diffusion with a spatially varying activation energy" proposed by Lee and coworkers.[24] They have shown that when the spacer layer thickness is small, i.e. the strain energy density wells are more intense and steeper, island nucleation can occur at the boundary of the tensilely strained region. In fact, as the adatoms approach the minimum of the strain energy density they drastically slow down and the for-

mation of stable island nuclei is promoted before the minimum is reached.

More work is necessary both experimentally and theoretically in order to establish the more appropriate model for the observed behavior.

Finally, we discuss another important difference between the two series that illustrates the effect of varying the stress intensity at the surface. Figure 4 shows that after 18 s deposition, the cluster diameters in the A and B samples are comparable, but the total volume of Ge islands in the cluster regions is significantly larger in the B case. This behavior implies that, upon reducing the spacer layer thickness, in the first stage of the growth either the island growth rate increases in the Si tensilely strained regions or the WL thickness decreases outside the cluster regions. In our opinion, the latter conclusion is favored by the data of Fig. 1(d), which show that, after 9 s of deposition, the Ge WL was grown mainly in the cluster regions. By assuming that the deposited material is the same in the samples of the two series, i.e., that the CVD surface reaction is not strongly influenced by the spacer layer thickness, it can be evaluated that the WL of the A series is 0.17 nm thicker (i.e., about 1 ML Ge) than the WL of the B series at this stage of the growth. This reduction of the WL thickness in the thinner spacer layer case is in good agreement with that reported by Schmidt *et al.* for similar spacer layer thickness and at a similar stage of the island growth process.[27]

On the basis of these observations, a stabilizing mechanism can be envisaged for the island dynamics that slows down the transition toward strained domes and creates the narrow distribution of sizes and shapes of the pyramids of Fig. 1(e). The possible mechanism could be: (i) islands nucleate and evolve to the stage of pyramids in the strained regions according to the SK mode; (ii) due to the increased island size, the repulsion from the pyramid edges become stronger and pushes the adatoms toward smaller pyramids inside the cluster or altogether away from the strain potential well, resulting in an island size stabilization similar to that described in Ref. 8. At a later deposition stage, a further growth of the WL outside the cluster regions is promoted, while the pyramids inside the clusters achieve size and shape uniformity. This growth dynamics is similar to that named SK2 by Daruka and Barabási in Ref. 1.

We have seen that in the series B samples, at a later growth stage [Figs. 1(f), 3(b), and 3(c)], after the transition from pyramids to domes, the islands are disposed within the clusters with a high degree of order. This evolution can be explained if we assume that, upon enlargement of the island size, in the restricted space of the strained regions a strong repulsive interaction between adjacent islands sets in that "pushes away" the island themselves along the "softer" [100]-[010] crystalline directions.[25] This repulsion, transmitted through the substrate, is enhanced in the cluster region because of the high island density and is more effective for domes rather than for pyramids, as we observe here. This is due to the higher stress that a strained dome induces on the substrate with respect to a pyramid. The strong dome-to-dome interaction, due to their small mutual separation within a cluster, impacts also on the dome size by reducing their base width of about 35%.

CONCLUSIONS

In conclusion, we have shown that, upon tuning the strain present on the Si(001) surface, the Ge island spatial distribution can be controlled to a remarkable extent. Ordered arrays of strain potential wells oriented along the [100]-[010] directions on the Si(001) surface were generated exploiting the self-ordering occurring in the growth of Ge island multilayers at 750°C. The intensity and shape of the strain potential wells were modified by changing the thickness of the topmost Si spacer layer.

The Ge islands on the surface, being deposited at 600°C and not capped by a silicon layer, have a typical size much smaller than the extension of the stress field at the surface. As a consequence, the formation of clusters made of few islands was observed.

Upon decreasing the topmost Si spacer layer thickness from 65 to 35 nm, we identified two different nucleation regimes. In the weak nucleation limit, the island growth is confined in cluster regions only for the first stage of their evolution (pyramids), while in the strong nucleation limit, the islands are assembled in clusters up to the last stage of their growth dynamics (relaxed domes). In the latter case, the strong stress arising from the template structure can modify the island growth dynamics. Our data suggest the occurrence of a modified SK growth that stabilizes the pyramids by slowing down the transition toward strained domes. Furthermore, island ordering along the [100]-[010] directions is observed within the clusters (*intracluster ordering*), due to elastic dipole repulsive interaction between adjacent islands. The strong dome-to-dome interaction impacts also on the dome size by reducing their base width of about 35%.

*Corresponding author; electronic address: capellini@fis.uniroma3.it

[1] I. Daruka and A.-L. Barabási, Phys. Rev. Lett. **79**, 3708 (1997).
[2] K. Brunner, Rep. Prog. Phys. **65**, 27 (2002).
[3] O. G. Schmidt, S Kiravittaya, Y. Nakamura, H. Heidemeyer, R. Songmung, C. Müller, N. Y. Jin-Phillipp, K. Eberl, H. Wawra, S. Christiansen, H Gräbeldinger, and H Schweizer, Surf. Sci. **514**, 10 (2002).
[4] T. I. Kamins, E. C. Carr, R. S. Williams, and S. J. Rosner, J. Appl. Phys. **81**, 1 (1997).
[5] L. Vescan, T. Stoica, O. Chretien, M. Goryll, E. Mateeva, and A. Mück, J. Appl. Phys. **87**, 7275 (2000).
[6] R. Loo, P. Meunier-Beillard, D. Vanhaeren, H. Bender, M. Caymax, W. Vandervorst, D. Dentel, M. Goryll, and L. Vescan, J. Appl. Phys. **90**, 2565 (2001).
[7] G. Capellini, M. De Seta, and F. Evangelisti, J. Appl. Phys. **93**, 291 (2003).
[8] A.-L. Barabási, Appl. Phys. Lett. **70**, 2565 (1997).

[9] O. G. Schmidt, O. Kienzle, Y. Hao, K. Eberl, and F. Ernst, Appl. Phys. Lett. **74**, 1272 (1999).
[10] S. A. Chaparro, Y. Zhang, J. Drucker, D. Chandrasekhar, and D. J. Smith, J. Appl. Phys. **87**, 2245 (2000).
[11] J. Tersoff, C. Teichert, and M. G. Lagally, Phys. Rev. Lett. **76**, 1675 (1996).
[12] F. Liu, S. E. Davenport, H. M. Evans, and M. G. Lagally, Phys. Rev. Lett. **82**, 2528 (1999).
[13] B. Yang, F. Liu, and M. G. Lagally, Phys. Rev. Lett. **92**, 025502 (2004).
[14] Q. Xie, A. Madhukar, P. Chen, and N. P. Kobayashi, Phys. Rev. Lett. **75**, 2542 (1995).
[15] G. Capellini, M. De Seta, F. Evangelisti, and C. Spinella. Appl. Phys. Lett. **82**, 1772 (2003).
[16] I. Daruka, A.-L. Barabási, S. J. Zhou, T. C. Germann, P. S. Lomdahl, and A. R. Bishop, Phys. Rev. B **60**, R2150 (1999).
[17] M. Meixner, E. Schöll, M. Schmidbauer, H. Raidt, and R. Köhler, Phys. Rev. B **64**, 245307 (2001).
[18] A. Hesse, J. Stangl, V. Holy, T. Roch, G. Bauer, O. G. Schmidt, U. Denker, and B. Struth, Phys. Rev. B **66**, 085321 (2002).
[19] G. Capellini, M. De Seta, and F. Evangelisti, Appl. Phys. Lett. **78**, 303 (2001); M. De Seta, G. Capellini, F. Evangelisti, and C. Spinella, J. Appl. Phys. **92**, 614 (2002).
[20] J. Stangl, A. Hesse, V. Holy, Z. Zhong, G. Bauer, U. Denker, and O. G. Schmidt, Appl. Phys. Lett. **82**, 2251 (2003).
[21] Th. Wiebach, M. Schmidbauer, M. Hanke, H. Raidt, R. Köhler, and H. Wawra, Phys. Rev. B **61**, 5571 (2000).
[22] Y. Kikuchi, H. Sugii, and K. Shintani, J. Appl. Phys. **89**, 1191 (2001).
[23] L. Vescan, K. Grimm, M. Goryll, and B. Holländer, Mater. Sci. Eng., B **69**, 324 (2000).
[24] C. -S. Lee, B. Kahng, and A.-L. Barabási, Appl. Phys. Lett. **78**, 984 (2001).
[25] V. A. Shchukin and D. Bimberg, Rev. Mod. Phys. **71**, 1125 (1999).
[26] R. Marchetti, F. Montalenti, and L. Miglio (private communication).
[27] O. G. Schmidt, O. Kienzle, Y. Hao, K. Eberl, and F. Ernst, Appl. Phys. Lett. **74**, 1272 (1999).